

# Lossy Compression of Natural HDR Content Based on Multi-Component Transform Optimization

Miguel Hernández-Cabronero\*, Victor Sanchez, Francesc Aulí-Llinàs and Joan Serra-Sagrìstà

**Abstract**—Linear multi-component transforms (MCTs) are commonly employed for enhancing the coding performance for the compression of natural color images. Popular MCTs such as the RGB to Y'CbCr transform are not optimized specifically for any given input image. Data-dependent transforms such as the Karhunen-Loève Transform (KLT) or the Optimal Spectral Transform (OST) optimize some analytical criteria (e.g., the inter-component correlation or mutual information), but do not consider all aspects of the coding system applied to the transformed components. Recently, a framework that produces optimized MCTs dependent on the input image and the subsequent coding system was proposed for 8-bit pathology whole-slide images. This work extends this framework to higher bitdepths and investigate its performance for different types of high-dynamic range (HDR) contents. Experimental results indicate that the optimized MCTs yield average PSNR results 0.17%, 0.47% and 0.63% higher than those of the KLT for raw mosaic images, reconstructed HDR radiance scenes and color graded HDR contents, respectively.

**Index Terms**—Image Compression, Multi-Component Transforms, HDR.

## I. INTRODUCTION

High dynamic range (HDR) contents offer enhanced contrast and extended color gamut by increasing the range of possible luminance values. Higher bitdepths are thus required to represent these data and the storage and transmission costs are increased, as compared to those of low dynamic range (LDR) contents. To alleviate these costs, some image and video coding methods have been proposed in the literature. These include standard compression algorithms (and approaches based thereon) such as JPEG [1], JPEG XT [2], JPEG2000 [3]–[5], H.264 [6] and HEVC [7] –e.g., the Main10 profile combined with the PQ BT.2020 non-linearity, and the screen content coding (SCC) extensions [8]. Ad-hoc algorithms have been proposed as well, based on the discrete wavelet transform (e.g., the PIZ encoder in OpenEXR [9]), the LogLuv transform [10], [11] and range-compression methods [12]–[14]. The compression of raw color filter array (CFA) data output by camera sensors –often employed to produce LDR data or to generate HDR content from multiple exposures [15]– has also been investigated in recent years [16]–[19].

This work has been funded by the EU Marie Curie CIG Programme under Grant PIMCO, the Engineering and Physical Sciences Research Council (EPSRC), UK, and by the Spanish Government (MINECO), FEDER, and the Catalan Government under Grants TIN2015-71126-R and 2014SGR-691.

\*M. Hernández-Cabronero and Victor Sanchez are with the University of Warwick, Coventry CV4 7AL, United Kingdom (e-mail: m.hernandez-cabronero@warwick.ac.uk).

F. Aulí-Llinàs and J. Serra-Sagrìstà are with the Universitat Autònoma de Barcelona, Bellaterra 08193, Spain.

It is a well known fact that linear multi-component transformations (MCTs) efficiently decorrelate the color components and compact the pixel energy, thus enhancing compression performance [20]. To the best of our knowledge, only data-independent MCTs are used in the aforementioned works. That is, each method applies only one MCT –e.g., the irreversible color transform (ICT) [3]–, normally designed for LDR data. Therefore, optimal decorrelation cannot be expected for any given input. On the other hand, data-dependent strategies apply different MCTs depending on the input to be compressed. Commonly, these MCTs are designed to minimize analytical criteria such as inter-component correlation or mutual information, hence yielding superior compression performance than data-independent MCTs. In general, methods based on Principal Component Analysis (PCA) –e.g., the Karhunen-Loève Transform (KLT)– and Independent Component Analysis (ICA) –e.g., the Optimal Spectral Transform [21] (OST)– provide highly competitive results. However, neither data-independent nor data-dependent MCTs take into account all details of the subsequent coding system applied to the transformed components, like the context models employed by the entropy coder. Hence, the resulting compression performance may also be suboptimal.

Recently, an optimization framework for obtaining MCTs dependent on the input data and the coding system was proposed for the compression of 8-bit pathology whole-slide images [22]. The optimized MCTs yielded by this framework significantly outperform the KLT and the OST, as well as other data-independent transforms. However, this framework has only been evaluated on LDR data. In this work, we propose a straightforward extension of this framework to higher bitdepths and investigate its MCT optimization efficiency for different types of natural –i.e., photography and video– HDR contents including reconstructed scene radiance, color-graded scenes and raw CFA mosaic images.

The rest of this paper is structured as follows. Section II describes the aforementioned optimization framework and its extension to HDR data. Experimental results are provided in Section III and Section IV draws conclusions and outlines future work.

## II. TRANSFORM OPTIMIZATION FOR HDR CONTENT

Any linear MCT for three-component images is fully described by a  $3 \times 3$  matrix  $M$  of real coefficients, which is applied independently to each pixel as follows:

$$(u, v, w)' = M(r, g, b)' \quad (1)$$

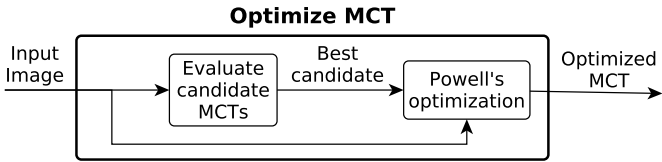


Fig. 1: Block diagram of the optimization framework in [22].

The MCT optimization framework proposed in [22], hereinafter referred to as OptimizeMCT, is designed to search for the matrix coefficients that minimize a cost function. This cost function evaluates the coding performance of a transform matrix by calculating a distortion metric between the original and the reconstructed image generated by a compression/decompression process using that MCT. Therefore, the obtained transform is optimized for that particular image and compression algorithm. In that work, image distortion is assumed to be the mean square error (MSE). Thus, the optimization is based on the energy of the reconstruction error, which is well understood and can be efficiently computed. Notwithstanding, this framework can be easily adapted to minimize any objective metric by modifying the cost function accordingly. A block diagram of OptimizeMCT is shown in Fig. 1. In the *Evaluate candidate MCTs* stage, the performance of a fixed set of MCTs including the KLT is evaluated for the input image and the best one is selected. In the *Powell's optimization* stage, the selected MCT undergoes a numerical optimization process. Powell's method [23] –similar to hill climbing optimization– iteratively modifies the 9 coefficients of the transform matrix and evaluates the resulting MCT.

Since the OptimizeMCT framework was originally conceived for LDR data, some modifications should be introduced so that it can be used for HDR contents. Firstly, the compression algorithm used in the cost function need be adapted for higher bitdepths. In [22] the transform matrices were evaluated using JPEG2000, which accepts arbitrary MCTs in Part 2 of the standard. Since bitdepths exceeding 16 bits per pixel (bpp) are supported, JPEG2000 is the compression algorithm of choice for this work as well. Hence, it suffices to adjust the input parameters related to the bitdepth to evaluate the OptimizeMCT framework for integer HDR data.

When contents are stored using floating-point samples –for instance, when using the OpenEXR format [9]– an additional preprocessing step is needed to convert them to integer values. The 16-bit IEEE 754-2008 float values typically employed in the OpenEXR format express smaller absolute values with higher precision than larger absolute values. Moreover, small values are much more probable than large values in typical camera footage and directly applying a 16 bit uniform quantizer to the input dynamic range may not represent HDR contents with enough fidelity. Based on the methodology proposed in [4], a normalized log function is applied to each input sample  $x$  before quantization,

$$y = \log_2(x - x_{\min} + 1), \quad (2)$$

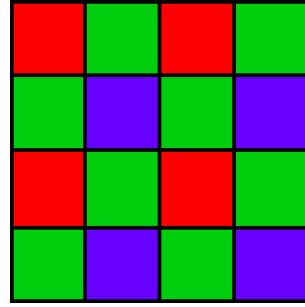


Fig. 2: A  $4 \times 4$  Bayer CFA pattern.

where  $x_{\min}$  is the lower bound of the dynamic range and the  $+1$  term is used to avoid negative and undefined values of  $y$ . As in [4], a uniform quantizer is then applied to map the resulting dynamic range  $[y_{\min}, y_{\max}]$  into unsigned 16-bit integers that can be processed by OptimizeMCT. Note that any other float to integer mapping can be evaluated in a similar way.

A special case of HDR data are the raw CFA mosaic images commonly employed for scene radiance reconstruction. Mosaic images contain only one component in which red, green and blue pixels are interleaved following a known pattern, typically the so-called Bayer CFA [24] depicted in Fig. 2. In this type of CFA, there are twice as many green pixels than red or blue pixels due to the higher sensitivity of the human visual system to green wavelengths. Therefore, a straightforward decomposition of the mosaic images into red, green and blue pixels yields components of heterogeneous dimensions that cannot be processed using linear MCTs as defined in (1). However, as described by Koh et al. [25], it is possible to obtain four color components of identical dimensions as follows:

$$\begin{bmatrix} r_{0,0} & G_{0,0} & r_{0,1} & G_{0,1} \\ g_{0,0} & b_{0,0} & g_{0,1} & b_{0,1} \\ r_{1,0} & G_{1,0} & r_{1,1} & G_{1,1} \\ g_{1,0} & b_{1,0} & g_{1,1} & b_{1,1} \end{bmatrix} \rightarrow \begin{bmatrix} r_{0,0} & r_{0,1} \\ r_{1,0} & r_{1,1} \end{bmatrix} \begin{bmatrix} G_{0,0} & G_{0,1} \\ G_{1,0} & G_{1,1} \end{bmatrix} \quad (3)$$

For images produced in this fashion, MCTs are defined by  $4 \times 4$  matrices. Therefore, Powell's optimization method needs be adapted to search in a 16-dimensional space, instead of the 9-dimensional space required for  $3 \times 3$  transforms. The compression algorithm used in the cost function must also be able to accept  $4 \times 4$  transform matrices. Since JPEG2000 supports images with multiple components, only simple changes in the input parameters are required to adapt OptimizeMCT to CFA mosaic images.

### III. EXPERIMENTAL RESULTS

A number of experiments are conducted to evaluate the performance of the OptimizeMCT framework for three types of HDR data. The first type are raw CFA mosaic images produced by Nikon camera sensors, with bitdepths of 12 and 14 bits. As discussed above, they can be employed to generate LDR content, or to produce data with larger

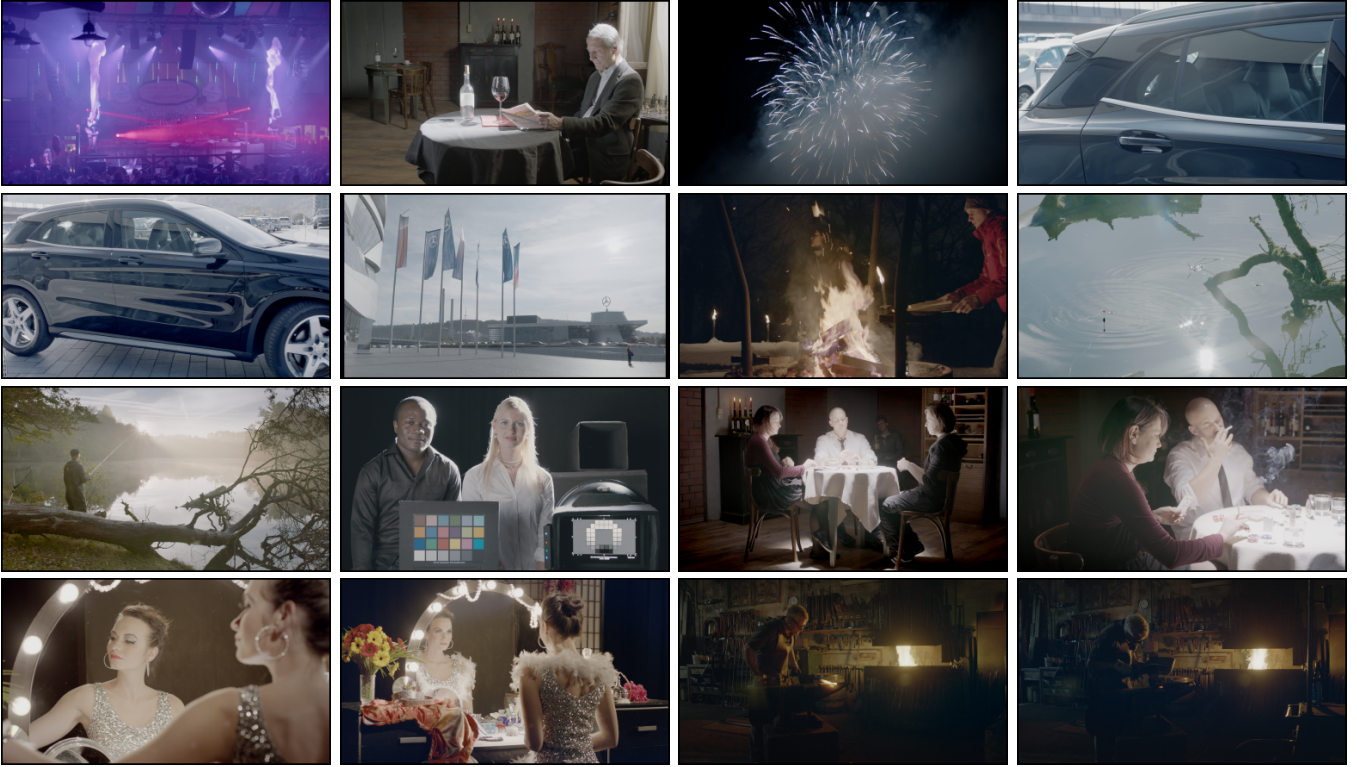


Fig. 3: Sample color-graded frames of the 16 sequences in the HdM-HDR-2014 set. From left to right and top to bottom: (1) Beerfest; (2) Bistro; (3) Carousel; (4) Cars close; (5) Cars full; (6) Cars long; (7) Fireplace; (8) Fishing close; (9) Fishing long; (10) Test image; (11) Poker full; (12) Poker traveling; (13) Showgirl 1; (14) Showgirl 2; (15) Hammering; (16) Welding.

dynamic ranges from multiple exposures. For this work, 20 real mosaic images of different color and edge complexity depicting portraits, landscapes and close shots are gathered [26] and split into four-component images as depicted in (3). The resulting images have dimensions ranging from  $3039 \times 2014$  to  $6080 \times 4012$ . This set is hereinafter referred to as *CFA mosaic*. The second content type are the 16 sequences of the scene radiance images of the HdM-HDR-2014 set [27]. Each frame was reconstructed from various exposures and needs to be processed before it can be displayed. Ten frames from each sequence, sampled uniformly across time, are considered for this work. The linear RGB pixels were originally stored using 16 bit IEEE 754-2008 floats, so they are mapped to 16 bit integers using (2) as described in Section II. The resulting 160 images are globally referred to as *HdM-HDR-2014 radiance*. The last type are the color-graded counterparts of the 160 *HdM-HDR-2014 radiance* images [27]. These images were graded for Rec.2020 primaries and  $0.005\text{-}4000\text{cd/m}^2$  luminance, and can be directly visualized using appropriate HDR displays. A sample frame from each sequence, tone-mapped to Rec.709, is shown in Fig. 3. This set, referred to as *HdM-HDR-2014 graded*, was originally distributed using 16 bit integer samples. Hence, no preprocessing is necessary. All images in the *HdM-HDR-2014 radiance* and the *HdM-HDR-2014 graded* corpora have dimensions equal to  $1920 \times 1080$ .

Two additional types of LDR content are also considered for the sake of comparison. The first type is referred to as *LDR standard* and contains 47 natural images from four popular corpora –the ISO CCITT set [28] (7 images), the ISO 12640-1 set [29] (8 images), the ISO 12640-2 set [30] (8 images) and the Kodak set [31] (24 images). Their dimensions range from  $512 \times 512$  to  $4096 \times 3072$ . The second type is referred to as *LDR WSI* and contains the 23 pathology whole-slide images (WSIs) of up to  $31655 \times 32619$  pixels with which the OptimizeMCT was originally evaluated [22]. All these LDR images are stored using 8-bit integers.

For each of the aforementioned images, the OptimizeMCT framework described in Section II is applied independently to produce an MCT. Each image is then compressed using Kakadu JPEG2000 v7.8 [32] with the corresponding optimized MCT and 5 levels of spatial discrete wavelet transform (DWT) decomposition. For comparison, each image is also compressed using four MCT matrices: the KLT, the identity matrix (i.e., no inter-component decorrelation), the JPEG2000 ICT [3] and the OST [21].<sup>1</sup> To evaluate each MCT, a single target bitrate  $R$  is defined for each image. Following the methodology in [22],  $R$  is set to  $R_{\text{ICT}}/2$ , where  $R_{\text{ICT}}$  is the highest compression rate achieved using JPEG2000 with the ICT and 5 spatial DWT levels. The images compressed using

<sup>1</sup>The OST was designed for the lossy compression of multicomponent images with JPEG2000.

the 5 aforementioned MCTs are then decompressed at their target bitrate, and each reconstructed version  $\hat{I}$  is compared to the original image  $I$  using the following PSNR definition:

$$PSNR(I, \hat{I}) = 10 \log_{10} \left( \frac{\max_I^2}{MSE(I, \hat{I})} \right) \quad (4)$$

$$MSE(I, \hat{I}) = \frac{1}{N} \sum_{i=1}^N |x_i - \hat{x}_i|^2. \quad (5)$$

Here,  $\max_I$  is the maximum value of  $I$ ,  $N$  is the total number of pixels in  $I$  and  $x_i$  and  $\hat{x}_i$  are, respectively, the  $i$ -th pixel of  $I$  and  $\hat{I}$ .

Average PSNR results for each MCT and corpus are provided in Table I. As obvious from the data, the OptimizeMCT framework produces transform matrices that outperform all other tested MCTs. On average, the optimized MCTs yield PSNRs 0.17%, 0.47% and 0.62% higher than the KLT for the *CFA mosaic*, the *HdM-HDR-2014 radiance* and the *HdM-HDR-2014 graded* sets, respectively. It should be noted that, although results in Table I are for a single target bitrate per image, improvements upon the KLT are obtained across low, medium and high bitrates. This can be observed in Fig. 4 for one sample image of each corpus.

The comparatively low performance achieved with the *CFA mosaic* corpus can be explained by the fact that pixels co-located in each of their four components were registered at different positions of the Bayer CFA array, as depicted in (3). Therefore, only a relatively low amount of inter-component correlation can be exploited. On the other hand, images from other corpora were produced by interpolating the red, green and blue samples of their corresponding mosaic images (not considered for this work), which results in more similar components. These results suggest that the the OptimizeMCT framework performs best when applied to sets of images with high inter-component redundancy. This hypothesis is consistent with the larger PSNR differences achieved for the LDR sets, whose images can only contain  $2^8$  different pixel values. As discussed in [22], WSI images exhibit significantly higher inter-component correlation than natural LDR images, due to the narrow range of colors present in WSIs. The different performance increments for the *LDR WSI* and *LDR standard* sets –i.e., respectively 6.09% and 4.15%– can be considered further evidence of our hypothesis. As can also be seen in Table I, high variability is present in the PSNR gains of the optimized MCTs over the KLT for sequences (1)-(16) of the *HdM-HDR-2014 radiance* and *HdM-HDR-2014 graded* corpora. Improvements lower than 0.1% are yielded for some sequences (e.g., *radiance* (4) Cars close and *graded* (12) Poker traveling), whilst other exhibit gains exceeding 1.3% (e.g., *radiance* (1) Beerfest) and 1.7% (e.g., *graded* (3) Carousel). As can be noticed by joint observation of Table I and Fig. 3, the sequences for which OptimizeMCT tend to produce the largest PSNR gains corresponds to the scenes with fewer color hues and lower brightness. Conversely, smaller PSNR increments are yielded for luminous scenes with higher color

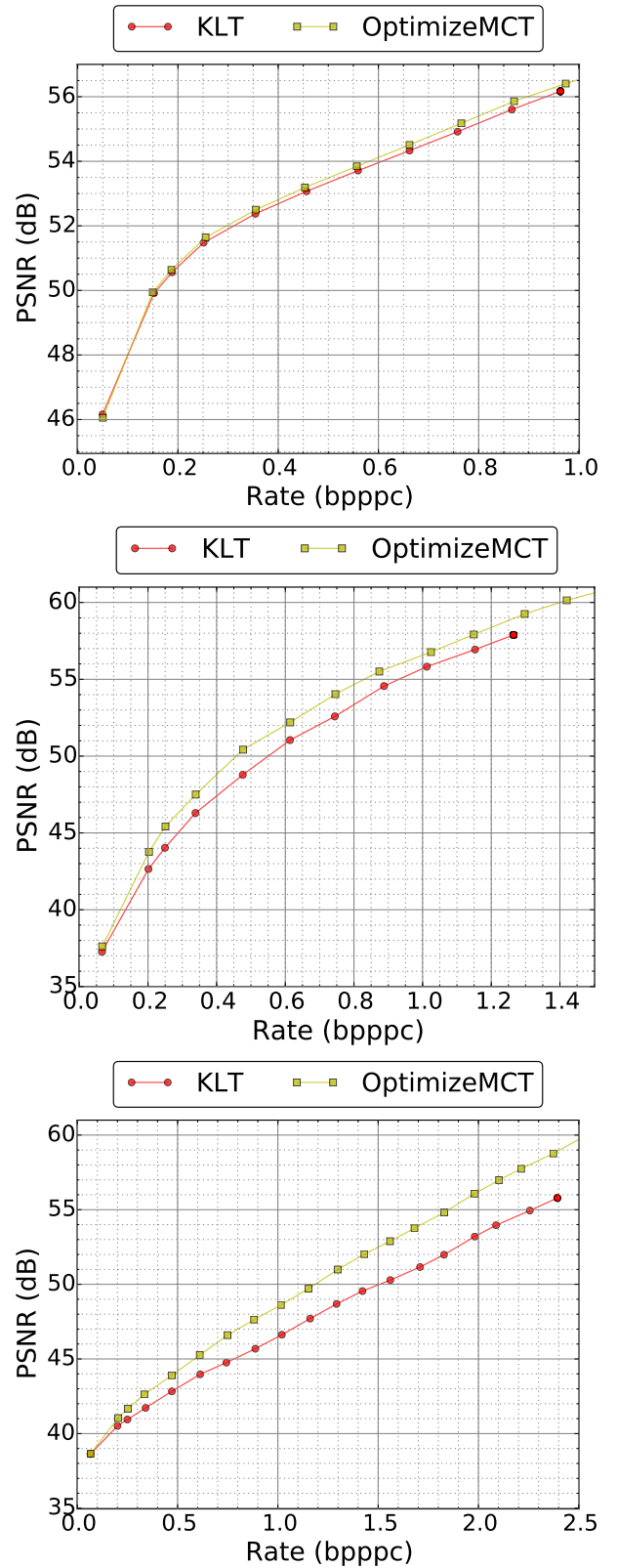


Fig. 4: Rate-distortion results for (top) the DS200 *CFA mosaic* image; (middle) a frame of the *HdM-HDR-2014 radiance* (1) Beerfest sequence; (bottom) a frame of the *HdM-HDR-2014 graded* (1) Beerfest sequence.

TABLE I: Average PSNR results in dB for different MCTs. Percentage differences with the KLT are provided between brackets, and the best results for each set are highlighted in bold font. Average target rates are expressed in bits per pixel per component.

Set name	Set	Bitdepth	Rate	KLT	No MCT	ICT	OST [21]	OptimizeMCT
<i>CFA mosaic</i>	20	12, 14	0.413	47.37	45.96 (-2.99%)	46.47 (-1.89%)	47.33 (-0.08%)	<b>47.45 (+0.17%)</b>
<i>HdM-HDR-2014 radiance</i>	160	16	0.554	49.37	43.75 (-11.39%)	48.00 (-2.77%)	48.85 (-1.05%)	<b>49.60 (+0.47%)</b>
(1) Beerfest	10	16	0.422	50.29	47.57 (-5.41%)	48.59 (-3.39%)	47.25 (-6.05%)	<b>50.95 (+1.31%)</b>
(2) Bistro	10	16	0.402	50.11	43.60 (-13.00%)	49.26 (-1.70%)	50.01 (-0.20%)	<b>50.18 (+0.14%)</b>
(3) Carousel	10	16	0.672	47.72	44.91 (-5.90%)	47.39 (-0.69%)	44.99 (-5.72%)	<b>48.00 (+0.58%)</b>
(4) Cars close	10	16	0.641	47.55	38.65 (-18.70%)	46.68 (-1.83%)	47.52 (-0.05%)	<b>47.59 (+0.09%)</b>
(5) Cars full	10	16	0.750	47.39	39.66 (-16.32%)	46.27 (-2.38%)	47.34 (-0.10%)	<b>47.47 (+0.17%)</b>
(6) Cars long	10	16	0.623	48.03	40.39 (-15.90%)	46.84 (-2.47%)	47.91 (-0.24%)	<b>48.09 (+0.14%)</b>
(7) Fireplace	10	16	0.596	49.54	46.21 (-6.73%)	47.64 (-3.83%)	48.51 (-2.07%)	<b>49.99 (+0.90%)</b>
(8) Fishing close	10	16	0.609	47.96	40.95 (-14.62%)	47.03 (-1.94%)	47.89 (-0.14%)	<b>48.09 (+0.28%)</b>
(9) Fishing long	10	16	1.178	45.57	37.88 (-16.87%)	44.20 (-3.02%)	45.54 (-0.06%)	<b>45.61 (+0.09%)</b>
(10) Test image	10	16	0.425	49.46	42.76 (-13.54%)	48.76 (-1.42%)	49.44 (-0.04%)	<b>49.59 (+0.26%)</b>
(11) Poker full	10	16	0.422	49.40	43.04 (-12.87%)	48.60 (-1.63%)	48.88 (-1.05%)	<b>49.46 (+0.12%)</b>
(12) Poker traveling	10	16	0.502	48.41	41.14 (-15.01%)	47.77 (-1.31%)	48.12 (-0.59%)	<b>48.61 (+0.42%)</b>
(13) Showgirl 1	10	16	0.604	50.15	44.70 (-10.86%)	47.35 (-5.58%)	49.56 (-1.19%)	<b>50.45 (+0.61%)</b>
(14) Showgirl 2	10	16	0.599	49.88	44.21 (-11.38%)	47.62 (-4.54%)	49.94 (+0.11%)	<b>50.12 (+0.48%)</b>
(15) Hammering	10	16	0.183	54.91	53.50 (-2.57%)	52.45 (-4.48%)	55.01 (+0.18%)	<b>55.41 (+0.91%)</b>
(16) Welding	10	16	0.230	53.53	50.77 (-5.16%)	51.59 (-3.62%)	53.72 (+0.36%)	<b>54.02 (+0.92%)</b>
<i>HdM-HDR-2014 graded</i>	160	16	0.962	44.86	44.17 (-1.55%)	44.65 (-0.46%)	44.03 (-1.86%)	<b>45.15 (+0.63%)</b>
(1) Beerfest	10	16	0.987	44.53	44.89 (+0.80%)	44.60 (+0.16%)	41.33 (-7.19%)	<b>45.17 (+1.44%)</b>
(2) Bistro	10	16	0.856	45.26	44.51 (-1.65%)	45.06 (-0.43%)	45.26 (+0.00%)	<b>45.39 (+0.28%)</b>
(3) Carousel	10	16	1.505	42.06	42.52 (+1.09%)	41.79 (-0.65%)	42.00 (-0.14%)	<b>42.79 (+1.73%)</b>
(4) Cars close	10	16	0.631	47.13	46.58 (-1.17%)	46.78 (-0.75%)	47.09 (-0.10%)	<b>47.25 (+0.25%)</b>
(5) Cars full	10	16	0.911	45.13	43.38 (-3.89%)	44.69 (-0.99%)	45.15 (+0.04%)	<b>45.23 (+0.22%)</b>
(6) Cars long	10	16	0.435	48.82	46.01 (-5.74%)	48.42 (-0.82%)	48.72 (-0.19%)	<b>48.87 (+0.11%)</b>
(7) Fireplace	10	16	1.105	43.10	43.16 (+0.15%)	43.13 (+0.07%)	40.07 (-7.02%)	<b>43.58 (+1.11%)</b>
(8) Fishing close	10	16	0.528	47.61	46.24 (-2.88%)	47.36 (-0.52%)	47.60 (-0.02%)	<b>47.66 (+0.11%)</b>
(9) Fishing long	10	16	0.863	45.07	42.11 (-6.58%)	44.74 (-0.73%)	45.10 (+0.05%)	<b>45.26 (+0.42%)</b>
(10) Test image	10	16	0.983	44.38	44.18 (-0.45%)	44.27 (-0.24%)	44.37 (-0.03%)	<b>44.63 (+0.55%)</b>
(11) Poker full	10	16	1.020	44.49	44.00 (-1.10%)	44.39 (-0.21%)	44.49 (+0.00%)	<b>44.66 (+0.38%)</b>
(12) Poker traveling	10	16	0.612	46.52	45.42 (-2.37%)	46.30 (-0.47%)	46.52 (-0.01%)	<b>46.55 (+0.06%)</b>
(13) Showgirl 1	10	16	0.991	43.84	44.03 (+0.43%)	44.24 (+0.90%)	42.82 (-2.34%)	<b>44.47 (+1.44%)</b>
(14) Showgirl 2	10	16	0.899	45.59	44.95 (-1.41%)	45.49 (-0.22%)	39.71 (-12.91%)	<b>45.81 (+0.47%)</b>
(15) Hammering	10	16	1.522	42.12	42.34 (+0.54%)	41.68 (-1.04%)	42.12 (+0.00%)	<b>42.50 (+0.91%)</b>
(16) Welding	10	16	1.541	42.14	42.39 (+0.59%)	41.52 (-1.47%)	42.14 (+0.00%)	<b>42.51 (+0.87%)</b>
<i>LDR standard</i>	47	8	1.171	42.51	39.82 (-6.33%)	43.76 (+2.93%)	39.71 (-6.59%)	<b>44.27 (+4.15%)</b>
<i>LDR WSI</i>	23	8	0.539	46.76	44.42 (-5.00%)	46.62 (-0.30%)	47.16 (+0.86%)	<b>49.61 (+6.09%)</b>

complexity. Again, this is consistent with the aforementioned hypothesis.

#### IV. CONCLUSIONS AND FUTURE WORK

Linear MCTs can significantly increase the coding performance for the compression of HDR contents. Traditional component transformations do not jointly take into account the statistical properties of the input image and all aspects of the coding system applied to the transformed components. Recently, an MCT optimization framework that tackles both aspects simultaneously was described for the compression of LDR content. This work proposes an extension of that framework, referred to as OptimizeMCT, to higher bitdepths and evaluates its performance for the compression of HDR contents.

Improved rate-distortion results as compared to the KLT are observed for the optimized MCTs for all tested sets. Average PSNR gains of 0.17%, 0.47% and 0.63% over the KLT are produced for CFA mosaic images, reconstructed HDR radiance scenes and HDR color graded scenes, respectively. Results

suggest that the the OptimizeMCT framework performs best for contents with redundant components, e.g., when a limited amount of hues are present.

Planned extensions to this work include MCT optimization based on distortion metrics better correlated with mean opinion scores such as the HDR-VDP-2 [33], and the evaluation of the optimized transform matrices using state-of-the-art video compression algorithms.

#### REFERENCES

- [1] G. Ward and M. Simmons, "JPEG-HDR: A Backwards-compatible, High Dynamic Range Extension to JPEG," in *ACM SIGGRAPH 2006 Courses*, Jul. 2006, pp. 1–8.
- [2] *JPEG XT*, ISO/IEC Std. 18477, 2014.
- [3] D. S. Taubman and M. W. Marcellin, *JPEG2000: Image compression fundamentals, standards and practice*. Kluwer Academic Publishers, Boston, 2002.
- [4] R. Xu, X. N. Pattanaik, and C. E. Hughes, "High-Dynamic-Range Still-Image Encoding in JPEG 2000," *IEEE Comput. Graph. Appl.*, vol. 25, no. 6, pp. 57–64, Nov. 2005.
- [5] T. Feng, S. Pal, and C. Abhayaratne, "Mapping-free high dynamic range image compression," in *International Conference on Consumer Electronics - Berlin, ICCE-Berlin*, Sep. 2015, pp. 172–175.

- [6] S. Liu, W.-S. Kim, and A. Vetro, "Bit-depth scalable coding for high dynamic range video," in *Visual Communications and Image Processing*, vol. 6822, 2008, pp. 68 2200–1 – 68 2200–10.
- [7] *High Efficiency Video Coding (HEVC), Recommendation ITU-T H.265, International Standard ISO/IEC 23008-2*, Std., apr 2013.
- [8] R. Joshi, J. Xu, D. Flynn, M. Naccari, C. Rosewarne, K. Sharman, J. Sole, G. Sullivan, T. Suzuki, Y. Wang *et al.*, "High Efficiency Video Coding (HEVC) Screen Content Coding: Draft 1," in *JCTVC-R1005, 18th JCT-VC meeting, Sapporo, JP*, 2014.
- [9] Industrial Light & Magic. Technical introduction to OpenEXR. [Online]. Available: <http://www.openexr.com/documentation.html>
- [10] G. W. Larson, "LogLuv encoding for full-gamut, high-dynamic range images," *Journal of Graphics Tools*, vol. 3, no. 1, pp. 15–31, 1998.
- [11] A. Motra and H. Thoma, "An adaptive LogLuv transform for High Dynamic Range video compression," in *IEEE International Conference on Image Processing, ICIP*, Sep. 2010, pp. 2061–2064.
- [12] R. Mantiuk, G. Krawczyk, K. Myszkowski, and H. P. Seidel, "High Dynamic Range Image and Video Compression - Fidelity Matching Human Visual Performance," in *IEEE International Conference on Image Processing, ICIP*, Sep. 2007, pp. I9–I12.
- [13] Y. Zhang, E. Reinhard, and D. Bull, "Perception-based high dynamic range video compression with optimal bit-depth transformation," in *IEEE International Conference on Image Processing, ICIP*, Sep. 2011, pp. 1321–1324.
- [14] S. Lasserre, F. L. Léanec, T. Poirier, and F. Galpin, "Backward compatible HDR video compression system," in *IEEE International Data Compression Conference, DCC*, Mar. 2016.
- [15] J. Kronander, S. Gustavson, G. Bonnet, and J. Unger, "Unified HDR reconstruction from raw CFA data," in *International Conference on Computational Photography, ICCP*, Apr. 2013, pp. 1–9.
- [16] A. Bazhyna and K. Egiazarian, "Lossless and near lossless compression of real color filter array data," *IEEE Trans. Consum. Electron.*, vol. 54, no. 4, pp. 1492–1500, 2008.
- [17] K.-h. Chung and Y.-h. Chan, "A Lossless Compression Scheme for Bayer Color Filter Array Images," *IEEE Trans. Image Process.*, vol. 17, no. 2, pp. 134–144, 2008.
- [18] D. Lee and K. N. Plataniotis, "Lossless compression of HDR color filter array image for the digital camera pipeline," *Signal Processing: Image Communication*, vol. 27, no. 6, pp. 637–649, 2012.
- [19] S. Kim and N. I. Cho, "Lossless Compression of Color Filter Array Images by Hierarchical Prediction and Context Modeling," *IEEE Trans. Circuits Syst. Video Technol.*, vol. 24, no. 6, pp. 1040–1046, Jun. 2014.
- [20] V. Goyal, "Theoretical foundations of transform coding," *IEEE Signal Process. Mag.*, vol. 18, no. 5, pp. 9–21, 2001.
- [21] I. P. Akam Bitra, M. Barret, and D. T. Pham, "On optimal transforms in lossy compression of multicomponent images with JPEG2000," *Signal Processing*, vol. 90, no. 3, pp. 759–773, 2010.
- [22] M. Hernández-Cabrero, F. Aulí-Llinàs, V. Sanchez, and J. Serra-Sagristà, "Transform Optimization for the Lossy Coding of Pathology Whole-Slide Images," in *IEEE International Data Compression Conference, DCC*, Mar. 2016.
- [23] J. Nocedal and S. Wright, *Numerical Optimization*, 2nd ed. Springer-Verlag New York, 2006.
- [24] B. Bayer, "Color imaging array," US Patent 3,971,065, Jul., 1976.
- [25] C. C. Koh, J. Mukherjee, and S. K. Mitra, "New Efficient Methods of Image Compression in Digital Cameras with Color Filter Array," *IEEE Trans. Consum. Electron.*, vol. 49, no. 4, pp. 1448–1456, 2003.
- [26] RawSamples.ch. (2015) Nikon Bayer CFA image set. [Online]. Available: <http://deic.uab.cat/~mhernandez/materials#bayer>
- [27] J. Froehlich, S. Grandinetti, B. Eberhardt, S. Walter, A. Schilling, and H. Brendel, "Creating cinematic wide gamut HDR-video for the evaluation of tone mapping operators and HDR-displays," in *IS&T/SPIE Electronic Imaging*. International Society for Optics and Photonics, 2014, pp. 90 230X–90 230X.
- [28] G. K. Wallace, "The ISO/CCITT standard for continuous-tone image compression," in *IEEE Global Telecommunications Conference and Exhibition, GLOBECOM*, vol. 1, Nov. 1989, pp. 564–568.
- [29] *Graphic technology - Prepress digital data exchange - Part 1: CMYK standard colour image data*, International Standard Organization (ISO) Std. 12 640-1, 1997. [Online]. Available: [http://www.iso.org/iso/catalogue\\_detail.htm?csnumber=40928](http://www.iso.org/iso/catalogue_detail.htm?csnumber=40928)
- [30] *Graphic technology - Prepress digital data exchange - Part 2: RGB encoded standard colour image data*, International Standard Organization (ISO) Std. 12 640-2, 2004. [Online]. Available: [http://www.iso.org/iso/catalogue\\_detail.htm?csnumber=33293](http://www.iso.org/iso/catalogue_detail.htm?csnumber=33293)
- [31] R. Franzen, "Kodak lossless true color image suite: PhotoCD PCD0992," 1999. [Online]. Available: <http://r0k.us/graphics/kodak/>
- [32] Kakadu JPEG2000 software. [Online]. Available: <http://www.kakadusoftware.com>
- [33] R. Mantiuk, K. J. Kim, A. G. Rempel, and W. Heidrich, "HDR-VDP-2: a calibrated visual metric for visibility and quality predictions in all luminance conditions," in *ACM Transactions on Graphics (TOG)*, vol. 30, no. 4. ACM, 2011, p. 40.